Measurement of nonuniform current densities and current kinetics in *Aplysia* neurons using a large patch method

Jon W. Johnson and Stuart Thompson
Hopkins Marine Station, Stanford University, Pacific Grove, California 93950

ABSTRACT A large patch electrode was used to measure local currents from the cell bodies of *Aplysia* neurons that were voltage-clamped by a two-microelectrode method. Patch currents recorded at the soma cap, antipodal to the origin of the axon, and whole-cell currents were recorded simultaneously and normalized to membrane capacitance. The patch electrode could be reused and moved to different locations which allowed currents from adjacent patches on a single cell to be compared. The results show that the current density at the soma cap is smaller than the average current density in the cell body for three components of membrane current: the inward Na current (I_{Na}), the delayed outward current (I_{out}), and the transient outward current (I_A). Of these three classes of ionic currents, I_A is found to reach the highest relative density at the soma cap. Current density varies between adjacent patches on the same cell, suggesting that ion channels occur in clusters. The kinetics of I_{out}, and on rare occasions I_A, were also found to vary between patches. Possible sources of error inherent to this combination of voltage clamp techniques were identified and the maximum amplitudes of the errors estimated. Procedures necessary to reduce errors to acceptable levels are described in an appendix.

INTRODUCTION

The processing of information by neurons is influenced by the characteristics of the various voltage-dependent ion channels that are expressed by the cell and the spatial distribution of the different channels. Macroscopic voltage clamp techniques are well suited for studying the collective properties of the ionic currents, and patch clamp methods allow investigation of single-channel properties. Neither method is particularly well suited to investigation of the absolute and relative densities of the various channel types in different regions of the cell; these are crucial parameters when extrapolating from channel properties to whole-cell behavior and for understanding the regional specialization of function within neurons.

We have begun to study the spatial distribution of ionic currents, and variability in the kinetics of currents, in defined regions of voltage-clamped *Aplysia* neurons. The method is adapted from the work of Frank and Tauc (1964) and Neher and Lux (1969). A large patch pipette is placed on an isolated, voltage-clamped neuron cell body, and simultaneous measurements are made of whole-cell currents and local currents in the patch of membrane covered by the pipette. In order to compare current densities in patch and whole-cell measurements, the currents are normalized to membrane capacitance. The experiments reported here demonstrate that the spatial distribution of Na and K currents on the cell body is not uniform, and that the kinetics of outward currents vary between patches on the same cell.

Dr. Johnson's present address is Laboratoire de Neurobiologie, École Normale Supérieure, 46, rue d'Ulm, 75230 Paris Cedex 05, France.
Address correspondence to Dr. Thompson.

METHODS

Specimens of *Aplysia californica* weighing 30–200 g were obtained from Sea Life Supply (Sand City, CA) and kept in flowing seawater at ocean temperature (11–15°C). Buccal ganglion B cells were chosen for study (Fiore and Meunier, 1979). The buccal ganglia were removed and manually desheathed and the hemiganglia were separated by a cut through the commissure. A group of neurons containing the B cell cluster was isolated by cutting all nerves at their point of exit and by removing the distal quarter of the hemiganglion. To reduce synaptic input, the cell bodies of the A interneurons and adjacent cells were removed by aspiration. The remaining clump of axotomized cells was 0.4–0.8 mm in diameter. We use the term "whole cell" to refer to the soma and initial axon remaining after this isolation procedure. The cells were bathed in a saline solution of the following millimolar composition: 476 NaCl, 39 $MgSO_4$, 24 $MgCl_2$, 10 $CaCl_2$, 10 KCl, 2 Hepes, pH 7.6–7.7. Bath temperature was maintained at 12°C.

Voltage clamp circuitry

The cells were voltage-clamped using a two-microelectrode method. Current and voltage microelectrodes were filled with 3 M KCl (resistance 2–5 MΩ) and inserted into the cell body. The bath was voltage-clamped to the ground potential using a separate voltage clamp amplifier connected to the bath via two saline-agar bridges. Whole cell current was measured from the voltage drop across a 500-kΩ resistor in series with the bath current electrode.

Currents were recorded from isolated patches of soma membrane using large diameter patch pipettes that were fashioned by a single pull,

0006-3495/89/02/299/10 $2.00

broken at the desired orifice diameter (5–50 μm), and lightly fire polished. Pipettes with a gradual taper were preferred because they were less likely to break into the cell. The orifice diameter that provided acceptable recordings most consistently was about 20 μm, corresponding to a resistance of about 300 KΩ. Gentle suction (10–50 cm of H_2O) was applied to the patch pipette to achieve a relatively high-resistance seal between the pipette and the membrane. The suction was maintained throughout the experiment. Higher seal resistances were obtained after treating the desheathed neurons with 0.2% trypsin (type IX, Sigma Chemical Co., St. Louis, MO) in normal saline for 30 min at 12°C (Westerfield and Lux, 1982; Siegelbaum et al., 1982). Using this procedure, seal resistances of 1–100 MΩ were achieved. After releasing the suction, the pipette could be removed and applied to an adjacent area of membrane. Patch recordings were always made from the hemisphere of the soma antipodal to the origin of the axon. We refer to this region as the soma cap.

The circuit used to control patch pipette potential and measure patch current is a simplified version of a standard patch clamp amplifier and employs a model 3528 operational amplifier (Burr-Brown Corp., Tucson, AZ) in current-to-voltage converter configuration with a 100-MΩ feedback resistor. Adequate bandwidth for our purposes was achieved with a simple circuit layout without frequency response correction. Capacitive transients could be fully charged through the feedback resistor, so that capacitive transient cancellation circuitry was unnecessary. Because cell voltage rather than pipette voltage was changed, the potential difference between the inside and outside of the patch pipette was always near zero and compensation for current loss across the seal resistance was not needed. Whole cell currents and patch currents were low-pass filtered at corner frequencies selectable between 30 and 4,000 Hz and photographed from the oscilloscope screen.

Measurement of membrane capacitance

To compare current densities in whole-cell and large patch measurements, the currents were normalized to membrane capacitance. This method is preferred because extensive infolding of the neuronal membrane makes a visual estimate of the area unreliable and because an unknown amount of membrane is aspirated into the patch pipette when suction is applied (Eaton, 1972; Mirolli and Talbott, 1972; Graubard, 1975). Membrane capacitance was measured by applying a triangle wave voltage command to the whole-cell voltage clamp and recording the resulting whole-cell and patch current waveforms (Fig. 1). Patch capacitance can be calculated directly from the change in the time derivative of voltage ($\Delta\, dV/dt$) at the vertex of a triangle wave and the corresponding jump in patch current (ΔI) from the equation:

$$c = \Delta I/(\Delta\, dV/dt)$$

(Neher, 1971; Palti, 1971). Because the voltage of the patch electrode is equal to the bath voltage and only the voltage across the membrane covered by the pipette is changing, the capacitance of the patch electrode should be rejected. To test this, the suction applied to the pipette was released and it was withdrawn about 100 μm from the membrane. The capacitance signal always decreased by a factor greater than 10 when the pipette was withdrawn, indicating that greater than 90% of the capacitance measured when the pipette is in contact with the cell is due to membrane capacitance.

Ideally, the capacitance of the whole cell could be measured with the same procedure, but this was more difficult in practice. Cell bodies were isolated as fully as possible; more drastic isolation caused injury resulting in low resting potentials and loss of action potential overshoot. The remnant of axon remaining after axotomy was several hundred micrometers in length. This is much less than the length constant of

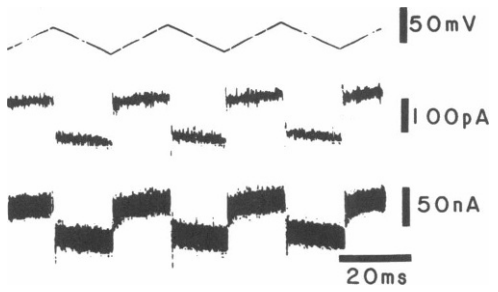

FIGURE 1 Measurement of patch and cell capacitance. The upper trace is cell voltage, the middle trace is patch current, and the lower trace is whole-cell current. Cell voltage is clamped to a triangle wave with an excursion from −40 to −80 mV at a frequency of 30 Hz. Jumps in capacitive current at each triangle wave vertex can be seen in both patch and whole-cell records. See Methods for details of the procedure used to estimate membrane capacitance. Patch current filtered at f_c = 2 kHz; whole-cell current unfiltered.

6–16 mm reported by Graubard (1975), although during depolarization the effective length constant of the axon will be shorter due to the greater membrane conductance. Axon spikes (Hagiwara and Saito, 1959) were sometimes seen during depolarizing pulses in the whole-cell current record, indicating that voltage was not always uniformly controlled. This complicates the measurement of whole-cell capacitance because the axonal capacitance is charged by the voltage clamp through an axial resistance. As a result, the whole-cell current during a triangle wave voltage command can exhibit three phases. The first phase, a large jump in capacitive current corresponding to the charging of soma capacitance, and the final phase, a straight line with a small slope due to current flowing across the membrane resistance, are of similar form in patch and whole-cell measurements. In the whole-cell record there may also be an intermediate phase characterized by a slight curvature. The curvature occurs because the nearly instantaneous change in dV/dt at the vertex of the triangle wave in the soma is spread out in time in the axon due to axial resistance in series with axonal capacitance. In the best cases, the whole-cell current showed a nearly instantaneous jump when the triangle wave changed sign and no intermediate curvature. This indicates good cell body isolation. Curvature was almost never seen in patch records except in rare instances in which the membrane was aspirated more than 100 μm into the patch pipette, creating an artificial axon. Such patches were not used.

The whole-cell capacitance was estimated by extrapolating the current recorded during phase 3 back to the time of the phase one jump. The change in current was measured from a point just before the triangle wave vertex to the level of the extrapolated line. This takes into account the slow change in capacitive current flowing in the axon and provides an improved estimate of cell capacitance. In most cells, the correction was less than 15% of the total capacitance. The largest correction was 30% of total capacitance. This is reasonable since a poorly isolated neuron (not used for this study because of its unusually large axon spikes) that was photographed after injecting the dye Lucifer Yellow (Stewart, 1978) had a neurite area equal to approximately 50% of the total membrane area, assuming uniform infolding.

In order to judge the accuracy of this approach, an electrical model of a cell body and axon was constructed and voltage-clamped to triangle wave commands like those used in experiments. The values used for membrane capacitance and resistance were derived from measurements on *Aplysia* cells. Axial resistance was calculated from the least favorable estimates of Graubard (1975) and the dimensions were measured from Lucifer Yellow–filled neurons. With a variety of equivalent axon

lengths, the current waveforms measured from the electrical model were remarkably similar to those recorded from cells. Even when 50% of the total cell capacitance was distributed in an axon with an equivalent length of 500 μm, 88% of the true capacitance was measured by this method. With shorter equivalent lengths, the accuracy greatly improved.

RESULTS

Currents measured in membrane patches at the soma cap during action potentials resemble the first derivative of intracellular voltage (dV/dt). Because capacitive current is proportional to dV/dt, while the ionic currents responsible for generating the action potential would flow in the opposite direction, this observation indicates that most of the current crossing the soma cap during the action potential is capacitive and that the action potential is generated elsewhere, either at the axon hillock or the proximal axon. Records of membrane voltage, patch current, and dV/dt during action potentials in three different cells are shown in Fig. 2. In Fig. 2, *A* and *B*, there is little difference between the patch current and dV/dt, suggesting that capacitive current overwhelms active ionic currents. This result is typical of the majority of cells. In Fig. 2 *C*, the patch current is slightly outward during the falling phase of the action potential, suggesting that in this patch, a significant outward current is activated during the spike.

The densities of ionic currents in the entire cell body and in large patches were measured in voltage clamp experiments. Three components of the current were separated using standard methods based on differences in voltage dependence and kinetics, as described in the legend to Fig. 3 (Adams et al., 1980). Example records of I_{Na} can be found in Fig. 7, of I_{out} in Figs. 4 *A* and 5; and of I_A in Fig. 4 *B*. Patch and whole-cell currents were scaled by membrane capacitance in order to estimate current densities. Cell capacitance ranged from 2.7 to 11.2 nF and patch capacitance was between 19 pF (patch pipette orifice diameter = 13 μm) and 327 pF (orifice diameter = 50 μm).

The bar graphs in Fig. 3 show examples of patch and whole-cell current densities in two different neurons and indicate that the soma cap region has a much lower density of I_{Na} and I_{out} than other regions of the soma and proximal axon. In these examples, the density of I_A is similar in the whole cell and patch measurements. The mean ratios of whole-cell current density to patch current density for 12 patches are given in Table 1. In each case the ratio is significantly greater than 1, indicating that the cap region has a relatively low density of channels. The only exception was that in two of the nine measurements of I_A, a higher current density was found at the soma cap than in the whole cell.

There was considerable variability in the ratio of whole-cell to patch current density, as evidenced by the large values obtained for the standard deviations in Table 1. This suggests that currents are not uniformly distributed in the soma. Spatial variation in current density was studied by comparing currents in several patches on the

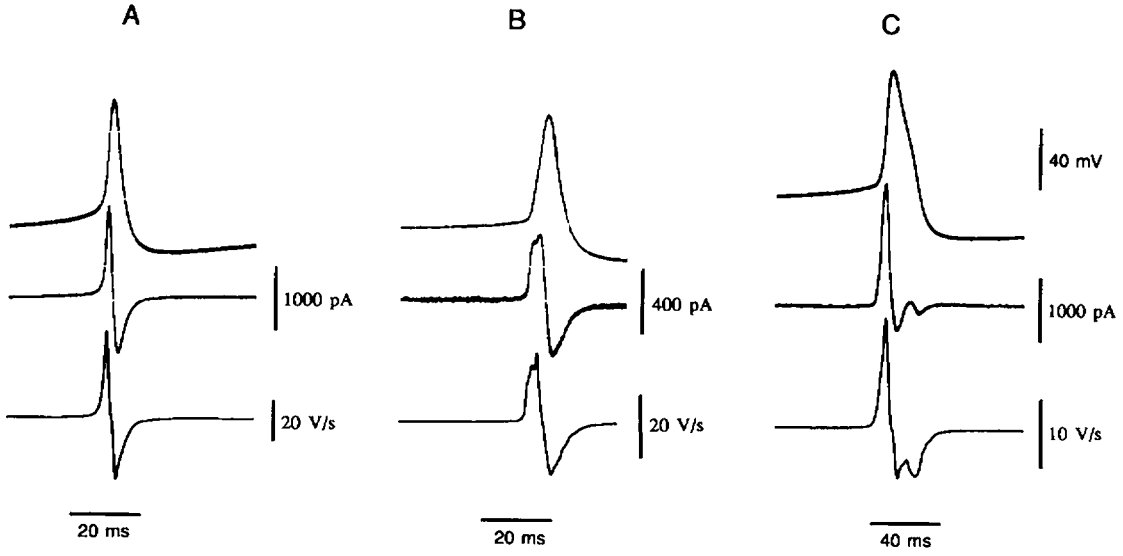

FIGURE 2 Membrane voltage, patch current, and the first derivative of membrane voltage (dV/dt) during action potentials in three neurons. The upper traces show membrane voltage recorded with an intracellular microelectrode in the soma. The middle traces are membrane currents measured simultaneously with a large patch electrode placed on the soma cap. The lower traces are dV/dt calculated from the measurements of membrane voltage.

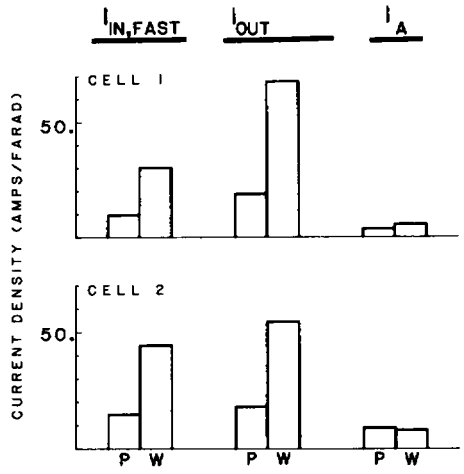

FIGURE 3 Comparison of current densities in a membrane patch at the soma cap (*P*) with the whole cell current densities (*W*) in two cells. The bar graphs show the current densities for each of three components of membrane current. I_{Na} was measured at the peak of the inward current transient during a voltage step from −40 to 0 mV (cell *2* and all cells used for Tables 1 and 2) or to +10 mV (cell *1*). Addition of 10 μM tetrodotoxin (TTX) to the bath produced a nearly complete block of the whole-cell inward current. With a delay of several minutes the patch inward current was also blocked, indicating that the TTX was diffusing into the patch pipette. The amplitude of I_{out} was measured 200 ms after a voltage step from −40 to +10 mV and results from a partial activation of both voltage-dependent, and Ca-dependent K currents (Thompson, 1977). I_A was measured at the peak of the outward current transient during a pulse to −20 mV after removing I_A inactivation with a 500-ms conditioning pulse to between −90 and −110 mV. Leakage current was estimated from the amplitude of the current during hyperpolarizing pulses from the −40-mV holding potential and subtracted from all other measurements.

same neuron. Table 2 gives the patch current densities for I_{Na}, I_{out}, and I_A in four patches at the soma cap. The current densities vary widely with the largest variation occurring in I_{out}. Similar patch-to-patch variability was observed in all of the experiments in which multiple patches on the same cell were compared.

TABLE 1 Ratio of whole-cell current density to patch current density, standard deviation of the ratio, and number of measurements

Current type	Ratio of current densities		
	W/P	SD	*n*
I_{Na}	9.5	4.3	8
I_{out}	5.0	2.2	9
I_A	2.4	1.6	9

Data gathered from 12 patches on five neurons in which all criteria for quantification of current density were met. All three ratios are significantly greater than one (I_{Na} and I_{out}, $P < 0.001$; I_A, $P < 0.025$; Student's *t* test). See legend of Fig. 3 for details of the measurement protocols.

TABLE 2 Patch capacitance and current densities for four patches from a single cell

Patch	Capacitance	I_{Na}	I_{out}	I_A
	pF		*pA/pF*	
1	31	3.2	7.4	0.56
2	38	4.2	6.9	1.3
3	30	3.7	12.0	1.3
4	28	4.3	22.3	0.71

See legend of Fig. 3 for details of the measurement protocols.

Kinetic differences

In several experiments the patch current followed a different time course than the whole-cell current. Fig. 4 *A* shows examples of outward currents recorded simultaneously in a patch located at the soma cap and in the whole cell. The whole-cell current reaches a peak and then inactivates during the depolarizing step as previously described (Aldrich et al., 1979), but the patch current continues to increase throughout the step. The Ca-dependent K current (I_C) may contribute to the gradually increasing outward current observed in the patch, but is unlikely to be the sole component of noninactivating outward current. This is because the large outward tail current after the return to the holding potential decays about 100 times faster than the I_C tail current in the whole cell under the conditions of this study (Thompson, 1977; Barish and Thompson, 1983; Thompson et al., 1986). The tail current in the patch decays at a rate similar to that of the voltage-dependent outward current, I_K (Adams et al., 1980). Tail currents with a time course typical of I_C were observed at the soma cap in three other patch experiments where the average I_C current density in the patch was 3.7-fold lower than the average whole-cell current density. The data in Fig. 4 *A* suggest that both inactivating and noninactivating components of voltage-dependent outward current are expressed simultaneously in the same cell.

Patch records of the transient K current, I_A, sometimes had a time course different from that of the whole-cell current. Simultaneous records from the whole cell and from a patch at the soma cap are compared in Fig. 4 *B*. In the patch, the peak current occurs later and the current decays more slowly than the whole-cell current, suggesting that the rates of I_A activation and inactivation in the patch are slower than the average rates in the whole cell. These differences were obtained over a wide range of prepulse voltages and I_A amplitudes, and it appears that they are due to differences in the kinetics of I_A rather than contamination from other currents activated by the depolarizing pulse.

Records from multiple patches on a single cell indicate

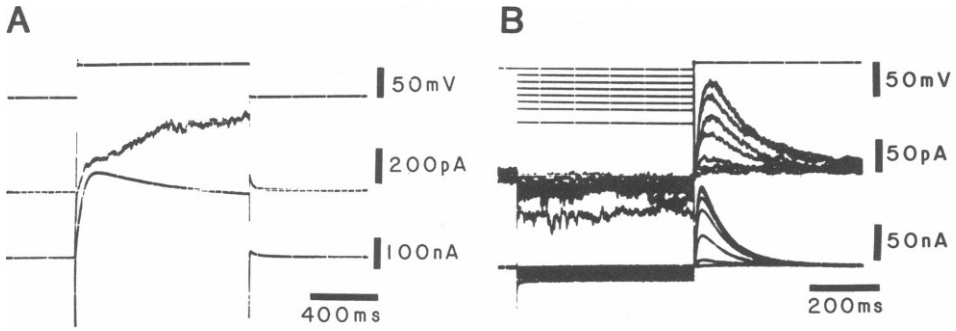

FIGURE 4 Comparison of whole-cell and patch outward current. Cell voltage is shown in the upper traces. Patch currents (middle traces) and whole-cell currents (bottom traces) were recorded simultaneously. (*A*) I_{out} during a 1-s pulse to +10 mV from a holding voltage of −40 mV. (*B*) I_A recorded during depolarizing pulses to −30 mV applied after a series of 500-ms conditioning pulses to voltages between −40 and −120 mV. Eight different sweeps are superimposed. The two sweeps exhibiting the largest I_A amplitude in the patch records overlap, as do the three sweeps with the largest I_A amplitude in the whole-cell records.

that the kinetic properties of currents at different locations near the soma cap are not uniform. Data from two patches on the same cell are compared in Fig. 5. Two 1-s pulses from −40 to +10 mV were presented with an interpulse interval of 1 s and the resulting currents were superimposed to illustrate the cumulative inactivation of delayed outward current (Aldrich et al., 1979). In Fig. 5 *A*, the delayed outward current in the patch inactivates at about the same rate as the whole-cell current and both records show cumulative inactivation. In Fig. 5 *B*, however, a nearby patch shows no inactivation during the same pulse sequence. It appears that at least some of the kinetic differences between whole-cell and patch currents illustrated in Fig. 4 *A* also occur between different patches on the same cell.

DISCUSSION

The combination of two-microelectrode voltage clamp with focal current recording using a large patch electrode allows detailed examination of the regional specialization of function within neurons. The principal advantages of the method are: (1) patch currents are recorded from a well-defined, limited area of membrane with low noise and high bandwidth; (2) voltage across the membrane patch is well controlled, resulting in fast settling of capacitive transients and allowing accurate current measurement at early times after a voltage step; (3) the current density, and the kinetics of currents, in the patch can be compared with macroscopic currents recorded

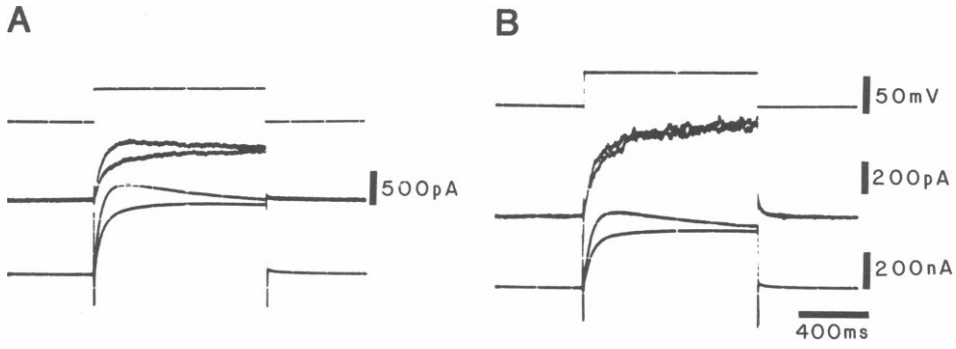

FIGURE 5 Comparison of outward currents in the whole cell and in two separate patches on the same neuron. Cell voltage appears in the upper trace, patch currents at the soma cap in the middle traces, and whole-cell currents in the lower traces. Currents were activated by a 1-s step to +10 mV from the holding voltage of −40 mV. The voltage was returned to −40 mV for 1 s and a second step to +10 mV was made. Currents recorded during the two voltage steps are superimposed. After the recordings in *A* were made, the patch pipette was removed and applied to an adjacent patch at the soma cap. Part *B* shows currents resulting from the same pulse sequence.

simultaneously from the whole cell; (4) several patches can be sampled from the same neuron.

Frank and Tauc (1964) first used this approach to study local membrane currents from voltage-clamped molluscan neurons and it has subsequently been used in several studies to record currents from restricted, well-clamped regions of the soma (e.g., Neher and Lux, 1979; Neher, 1971; Eckert and Lux, 1976; Westerfield and Lux, 1982). A modification of the method introduced by Strickholm (1961) was used to measure currents from patches on skeletal muscle cells (Almers et al., 1983). In this "loose patch clamp" method, the patch voltage rather than the cell voltage is changed. The large currents that flow across the seal resistance of the patch electrode in this configuration require elaborate compensation or an electrically guarded concentric patch pipette (Stuhmer et al., 1983; Almers et al., 1984). The method allows measurement of local membrane current and estimation of channel density in cells that cannot be voltage clamped effectively by other techniques.

Heterogeneity in current density

The nonhomogeneous distribution of membrane currents in molluscan neurons was suggested by several studies. A relatively low density of transient inward current in the soma was observed using a combination of intracellular and extracellular electrodes to gauge current density (Tauc, 19762a, b) as well as by using large patch electrodes on voltage-clamped cells (Frank and Tauc, 1964; Neher, 1971). Delayed outward currents were observed to reach larger amplitudes than inward currents, suggesting that the soma is predominantly a source of potassium current (Neher, 1971; Neher and Lux, 1971). Kado (1973) used a differential pair of external voltage electrodes to estimate local current amplitudes and found that the Na current is larger in the axon than in the soma whereas Ca and K currents are larger in the soma. A higher Ca current density in the soma relative to the axon was also suggested by Horn (1978) and by Standen (1975). Thompson and Coombs (1988) used the method described here to measure Ca current density in the soma and found that it is lowest near the soma cap and increases as the axon hillock is approached.

The current densities of I_{Na}, I_{out}, and I_A were, with few exceptions, significantly lower in patches at the soma cap than the average current densities in the axotomized cell body. Because whole-cell measurements were made from neurons axotomized to within several hundred micrometers of the soma, these data suggest that higher channel densities are to be found near the axon hillock or the initial segment of the axon. The difference in current density was greatest for I_{Na} and it appears that the density of I_{Na} at the soma cap is so low that this region does not contribute significantly to the generation of action potentials. This is shown by the fact that during the rising phase of the action potential the current was always outward in patch records from the soma cap, a result that is consistent with the earlier findings of Tauc (1962a, b) and Neher (1971).

There is some uncertainty in the measurements of I_{Na} in the whole cell because of incomplete control of axonal membrane voltage. A regenerative response in the axon could depolarize axonal membrane to a voltage greater than the command voltage and lead to overestimation of the amplitude of the whole cell inward current. However, the overestimate could not be very large. In membrane patches, a step of 0 mV activates I_{Na} to two-thirds of its maximum amplitude. If there were complete escape in the axon during the step to 0 mV, the apparent amplitude of the whole-cell current would be at most 1.5 times the true value. The larger ratio of whole-cell/patch inward current density in Table 1 makes it clear that the density of inward current channels is many times lower at the soma cap than elsewhere on the axotomized neuron.

The measurements of I_{out} and I_A in the whole cell are subject to less uncertainty because outward currents do not cause regenerative escape and because measurements of outward current are made at later times when the membrane capacitance is fully charged. For I_A, the ratio of whole-cell/patch current density was significantly smaller than for either I_{Na} ($P < 0.04$, Behrens-Fisher t test (Snedecor, 1956)) or I_{out} ($P < 0.02$) indicating that the soma cap is enriched in I_A relative to the other currents. In two out of nine experiments, the I_A density was higher at the soma cap than in the whole cell. I_A has a strong influence on the interspike interval during repetitive firing (Connor and Stevens, 1971) and these results suggest that the soma membrane plays a more significant role in the modulation of firing rate than in action potential generation.

Large patch recording reveals local nonuniformities in the distribution of ionic currents in *Aplysia* neurons. There was much greater variability in current density between different patches on the same cell than would be expected if channels were randomly distributed. For example, the four measurements of I_A density in Table 2 give a mean ± SD of 0.97 ± 0.39 pA/pF. Because the patch electrode samples a small fraction of the total cell surface, the Poisson distribution can be used to estimate the expected SD of channel number if their distribution were random. Assuming a single channel conductance of 14 pS (Taylor, 1987), an open probability of 0.5, and a driving force of 60 mV at −20 mV (Brown and Kunze, 1974), the mean current density corresponds to a minimum of 64 channels in the smallest of the four patches. The SD expected from the Poisson distribution is 8, while the observed SD corresponds to 26 channels. Similar

calculations for the measurements of I_{out} in Table 2 indicate an even larger deviation from random distribution, although in this case the interpretation is complicated by the possible contribution of different channel types. The results suggest that the potassium channel distribution is far from uniform and are consistent with the idea that potassium channels occur in multichannel aggregates, as has been suggested for I_A (Taylor, 1987). Nonrandom channel distributions have also been observed for I_{Na}, and to a lesser extent I_K, in frog skeletal muscle (Almers et al., 1983) and for Ca channels in molluscan neurons (Thompson and Coombs, 1988). It appears that clustering of ion channels may be a general phenomenon (Almers and Stirling, 1984; Poo, 1985). These results suggest that mechanisms exist to regulate the insertion and anchoring of ion channels into particular regions of the cell. Such mechanisms can have a great influence on neuronal function.

Heterogeneity in kinetics

In some experiments there were clear differences in the kinetics of whole-cell and patch outward currents. This was particularly striking for I_{out}. Cumulative inactivation of the delayed outward current was always seen in the whole-cell records while patch currents often grew steadily without inactivating during long depolarizations. I_{out} exhibited different inactivation kinetics in adjacent patches on the same cell. The variability in kinetics suggests that a single neuron may express two or more species of voltage-dependent K channels, some showing strong inactivation and others little or none (Llano and Bezanilla, 1985; Strong and Kaczmarek, 1986; Ram and Dagan, 1987).

Differences in the kinetics of I_A between the patch and the whole cell were rare, but when present the difference persisted over a wide range of current amplitudes, indicating that contamination from other currents was not the cause. Evidence for cellular differences in the kinetics of I_A has been found in several preparations, including molluscan neurons (Serrano, 1982), and at the single-channel level in *Drosophila* neurons and muscle cells (Solc et al., 1987).

APPENDIX

The large-patch method for recording local current density is subject to several potential errors. Some sources of error are inherent to any patch clamp method; relevant discussions of patch clamp and loose patch techniques can be found in Sakmann and Neher (1983). Other error sources are due to interactions between the whole-cell and patch clamp circuits. Because the waveform of the patch current often resembles the whole-cell current, the pickup of a fraction of the whole cell current by the patch circuit could represent a serious artifact that might easily be overlooked. A description of the five most important sources of error follows, along with estimates of their worst-case magnitudes and the methods used to reduce errors to acceptable levels. This section makes reference to the schematic diagram in Fig. 6; the symbols are defined in the figure legend.

Inadequate control of cell voltage

The gain of voltage clamp amplifiers is usually sufficient to keep the magnitude of the membrane voltage error acceptably small. However, when the current, and thus the membrane voltage error, changes quickly, a significant current can flow across the capacitance of the membrane patch and be measured by the patch clamp amplifier. The error current is:

$$I_e = C_{mp}(dV_{me}/dt).$$

The definition of open loop gain, $V_{me} = -V_0/A$, can be differentiated to replace dV_{me}/dt if A is assumed to be time independent. Assuming that R_{ei} is constant, and noting that when the cell is voltage-clamped to a constant command voltage, V_0 changes much more quickly than V_m, the following approximation can be made:

$$dV_0/dt = (dI_m/dt)\,R_{ei}.$$

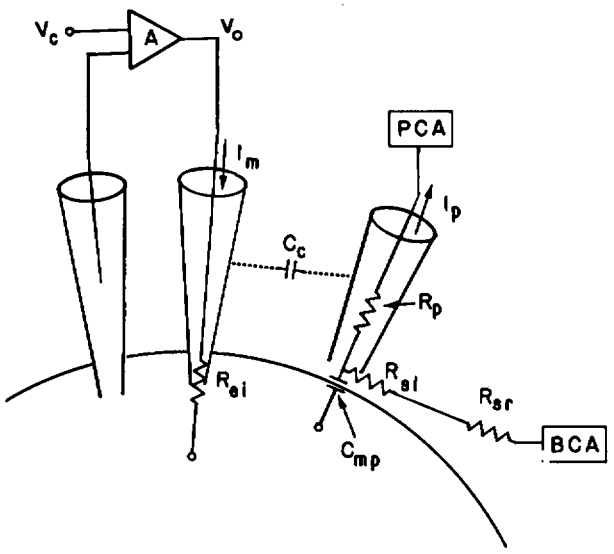

FIGURE 6 Schematic diagram of a cell with voltage clamp electrodes and the large patch pipette in place. The symbols used in the figure and in the text are as follows: A, voltage clamp open loop gain; BCA, bath clamp amplifier; C_c, coupling capacitance between voltage clamp current electrode and patch electrode; C_{mp}, capacitance of membrane patch; I_e, current error; I_m, membrane current supplied by voltage clamp; I_p, patch membrane current supplied by patch clamp amplifier; R_{ei}, resistance of voltage clamp current electrode; R_p, axial resistance of patch electrode; R_{sl}, resistance of seal between patch pipette and cell membrane; R_{sr}, series resistance between the outside of the patch electrode and BCA; V_c, voltage clamp command voltage; V_e, voltage error at tip of the patch pipette; V_{me}, membrane voltage error (membrane voltage minus command voltage); V_0, voltage clamp output voltage.

This equation does not hold during capacitance measurements, but in that case dV_0/dt is small and the error is insignificant. From these equations the current error due to capacitive current in the patch during changes in membrane voltage error can be approximated by:

$$I_e = -C_{mp}R_{ei}(dI_m/dt)/A.$$

We minimized this error by using low-resistance microelectrodes and by configuring the voltage clamp amplifier so that it had a high open loop gain ($\sim 4 \times 10^5$) at low frequencies. Such a high gain results in damped oscillations for 0.1–1 ms after large voltage steps but the oscillations do not interfere with the measurements described here. The gain of the amplifier, A, is frequency dependent because of the limited bandwidth of operational amplifiers. The open loop gain at 1 kHz (near the highest frequency at which dI/dt in these cells has significant power) is approximately 50,000. Using this value for A, the most rapidly changing whole-cell current (1 mA/s), and a large value for current microelectrode resistance (10 mΩ), the maximum error (normalized to C_{mp}) is calculated to be 0.2 pA/pF. An error of this magnitude would occur only while the whole cell current is changing rapidly, and made no significant contribution to the measurements reported here.

Capacitive coupling between electrodes

Capacitive coupling between the current electrode of the voltage clamp and the patch pipette can produce an artifactual patch current. Using the approximation of dV_0/dt given above, the magnitude of the current error is:

$$I_e = C_c R_{ei}(dI_m/dt).$$

The coupling capacitance was measured by driving the voltage clamp current electrode with a triangle wave of about 100 V peak-to-peak amplitude and monitoring the current jump in the patch electrode when the triangle wave changes sign (see Methods). When the electrodes are not shielded from each other, the coupling capacitance can be over 100 fF, which produces a large error. By inserting a grounded copper plate between the current and patch electrodes, and by paying careful attention to the experimental layout, the coupling capacitance can be reduced to about 1 fF. The cell voltage electrode and the patch pipette are placed on the same side of the shield, opposite the cell current electrode. The shield also serves to reduce coupling between the current and voltage electrodes of the voltage clamp, allowing higher voltage clamp gain and reducing high-frequency noise in the whole-cell current record. Assuming a coupling capacitance of 1 fF and the values given above, the worst case error is 10 pA. It should be noted that the two error sources described above depend on the current electrode resistance which may change when large currents are flowing. Using low resistance current electrodes helps to minimize this problem.

Series resistance in the bath

A third kind of error occurs when the voltage outside the patch pipette changes due to current flowing in the series resistance between the membrane and the input to the bath ground or virtual ground (R_{sr}). The error current across R_{sr} is given by:

$$I_e = I_m R_{sr}/R_{sl}.$$

R_{sr} is the sum of the series resistances of the bath, the agar bridge, and the liquid-silver chloride junction at the bath electrode. Since the epineural sheath is removed and the cells are immersed in a highly conductive saline, the series resistance of the bath is small, but the resistance of the agar bridge and the bath electrode is typically several kΩ. The error due to series resistance can be reduced by measuring the bath voltage with a separate electrode and substracting it from both the patch voltage reference and the membrane voltage input to the voltage clamp. Instability can result, however, if the bath voltage is measured with a greater bandwidth than the membrane voltage. This is commonly remedied by decreasing the bandwidth of the bath voltage follower, an approach that degrades the performance of the voltage clamp and can produce other sources of error. The solution we used, which eliminates the need to subtract the bath voltage at the other circuits, was to voltage clamp the bath using an independent clamp amplifier. Two separate agar bridges and silver chloride pellets were used to measure bath voltage and to pass current to the bath. Because of the low resistances of these electrodes, a simple but very fast bath clamp circuit can be constructed from a single operational amplifier (a Harris Corp. model 5110 was found to work well). This circuit holds the bath voltage to within 0.5 mV under all conditions except for an excursion of a few millivolts lasting less than 50 μs after very large voltage steps. A differential amplifier was used to measure the whole-cell current from the voltage drop across a 500 kΩ resistor in series with the bath current electrode.

The remaining series resistance was estimated from the equation described above by measuring whole cell and patch currents during the production of axon spikes with R_{sl} left intentionally low. Since axon spikes cannot occur in a soma membrane patch, a rapidly changing current recorded by the patch amplifier during the axon spike must be equal to I_e. R_{sr} was found to have a value of about 100 Ω under these conditions. A maximum error of 30 pA was calculated using this value, a seal resistance of 1 MΩ (the minimum accepted during experiments), and a whole-cell current amplitude of 300 nA. An error of this magnitude would occur only when a large pipette with a low seal resistance is used and when large currents are flowing. In practice, the error was insignificant even when the current density in the patch was only 10% of that in the whole cell.

Current flowing across the seal resistance

The error resulting from current flowing in the seal resistance between the patch pipette and the bath can be calculated from the equation:

$$I_e = I_p R_p/(R_p + R_{sl}).$$

The seal resistance was improved by treating the cells with trypsin and by applying suction to the patch pipette as described in Methods. With this procedure, seal resistances greater than 100 times the axial resistance of the patch pipette were often achieved. Data were not accepted unless ($R_p + R_{sl}$) was at least 10 times R_p, so this error was limited to a maximum of 10%. We found it necessary to maintain suction on the patch pipette throughout the experiment in order to maintain the seal resistance. This sometimes resulted in a gradual increase in patch area as membrane was slowly pulled into the pipette. In order to control for the changing membrane area, it was necessary to make current and capacitance measurements as close together in time as possible. The application of suction sometimes caused the resting conductance of the patch to increase abruptly, suggesting that the membrane had ruptured. Surprisingly, patch conductance often recovered when the suction was released and the cell appeared undamaged. A possible explanation is that stretch-activated channels may be opened by membrane deformation during the application of suction (Guharay and Sachs, 1984; Sigurdson et al., 1987). The sudden development of high patch conductance was the most common cause for rejecting a patch from further study.

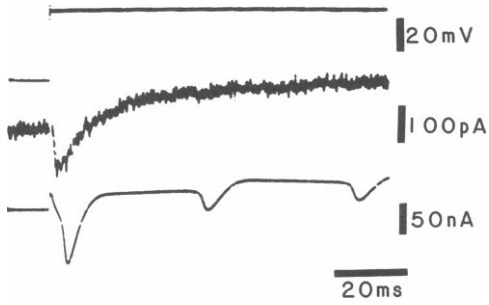

FIGURE 7 Absence of axon spikes in large patch current measurements. The upper trace is cell voltage, the middle trace is patch current, and the lower trace is whole-cell current. After a step from −40 to 0 mV, a transient inward current is seen in both the whole-cell and patch records. Subsequent inward transients in the whole cell record which result from uncontrolled spikes in the axon are rejected in the patch recording.

Axial resistance of the patch electrode

A final source of error is the voltage drop that results from current flowing in the access resistance of the patch pipette. With a typical patch electrode resistance of 300 kΩ and maximum patch current of 500 pA, the resulting voltage error is 0.15 mV, an insignificant error in these experiments.

In summary, the major errors inherent to the large patch current recording method can be reduced to acceptable levels by increasing the gain and bandwidth of the microelectrode voltage clamp, by using low resistance voltage clamp electrodes, by paying careful attention to experimental layout, by ensuring good control over bath voltage, and by achieving a reasonably high seal resistance. The first three errors described above are difficult to quantify but the conclusion that these errors are reduced to acceptable levels is supported by direct observation. If these errors were significant, an artifactual current that depends on the amplitude of the whole cell current would be recorded by the patch electrode, especially when the whole cell current changes rapidly. The observation that axon spikes appearing in the whole-cell record are consistently rejected in the patch current record (Fig. 7) supports the conclusion that such artifacts were successfully eliminated.

We thank P. Ascher for helpful comments and the staff of the Hopkins Marine Station, Pacific Grove for support.

This research was supported by U.S. Public Health Service grant NS14519 to Dr. Thompson and predoctoral NRSA MH 09113 to Dr. Johnson.

Received for publication 11 April 1988 and in final form 23 September 1988.

REFERENCES

Adams, D. J., S. J. Smith, and S. H. Thompson. 1980. Ionic currents in molluscan soma. *Annu. Rev. Neurosci.* 3:141–167.

Aldrich, R. W., P. A. Getting, and S. H. Thompson. 1979. Inactivation of delayed outward current in molluscan neurone somata. *J. Physiol. (Lond.).* 291:507–530.

Almers, W., W. M. Roberts, and R. L. Ruff. 1984. Voltage clamp of rat and human skeletal muscle: measurements with an improved loose-patch technique. *J. Physiol. (Lond.)* 347:751–760.

Almers, W., P. R. Stanfield, and W. Stuhmer. 1983. Lateral distribution of sodium and potassium channels in frog skeletal muscle: measurements with a patch-clamp technique. *J. Physiol. (Lond.)* 336:261–284.l

Almers, W., and C. Stirling. 1984. Distribution of transport proteins over animal cell membranes. *J. Membr. Biol.* 77:169–186.

Barish, M. E., and S. H. Thompson. 1983. Calcium buffering and slow recovery kinetics and calcium-dependent outward current in molluscan neurones. *J. Physiol. (Lond.).* 337:201–219.

Brown, A. M., and D. L. Kunze. 1974. Ionic activities in identifiable *Aplysia* neurons. *Adv. Exp. Med. Biol.* 50:57–73.

Connor, J. A., and C. F. Stevens. 1971. Prediction of repetitive firing behaviour from voltage clamp data on an isolated neurone soma. *J. Physiol. (Lond.)* 213:31–53.

Eaton, D. C. 1972. Potassium ion accumulation near a pace-making cell of *Aplysia*. *J. Physiol. (Lond.)* 224:421–440.

Eckert, R., and H. D. Lux. 1976. A voltage-sensitive persistent calcium conductance in neuronal somata of *Helix*. *J. Physiol. (Lond.)* 254:129–151.

Fiore, L., and J.-M. Meunier. (1979). Synaptic connections and functional organization in *Aplysia* buccal ganglia. *J. Neurobiol.* 10:13–29.

Frank, K., and L. Tauc. 1964. Voltage-clamp studies of molluscan neuron membrane properties. *In* The Cellular Function of Membrane Transport. J. Hoffman, editor. Prentice Hall, Inc., Englewood Cliffs, NJ. 113–135.

Graubard, K. 1975. Voltage attenuation within *Aplysia* neurons: the effect of branching pattern. *Brain Res.* 38:325–332.

Guharay, F., and F. Sachs. 1984. Stretch-activated single ion channel currents in tissue-cultured embryonic chick skeletal muscle. *J. Physiol. (Lond.).* 352:685–701.

Hagiwara, S., and N. Saito. 1959. Voltage-current relations in nerve cell membrane of *Onchidium verruculatum*. *J. Physiol. (Lond.).* 148:161–179.

Horn, R. 1978. Propagating calcium spikes in an axon of *Aplysia*. *J. Physiol. (Lond.)* 281:513–534.

Kado, R. T. 1973. *Aplysia* giant cell: soma-axon voltage clamp current differences. *Science (Wash. DC).* 182:843–845.

Llano, I., and F. Bezanilla. 1985. Two types of potassium channels in the cut-open squid giant axon. *Biophys. J.* 47:221*a*. (Abstr.)

Mirolli, M., and S. R. Talbott. 1972. The geometrical factors determining the electrical properties of a molluscan neurone. *J. Physiol. (Lond.).* 227:19–34.

Neher, E. 1971. Two fast transient current components during voltage clamp on snail neurons. *J. Gen. Physiol.* 58:36–53.

Neher, E., and H. D. Lux. 1969. Voltage clamp on *Helix pomatia* neuronal membrane; current measurement over a limited area of the soma surface. *Pflügers Arch.* 311:272–277.

Neher, E., and H. D. Lux. 1971. Properties of somatic membrane patches of snail neurons under voltage clamp. *Pflügers Arch.* 322:35–38.

Palti, Y. 1971. Varying potential control voltage clamp of axons. *In* Biophysics and Physiology of Excitable Membranes. W. F. Adelman, Jr., editor. Van Nostrand Reinhold Company, 194–205.

Poo, M.-M. 1985. Mobility and localization of proteins in excitable membranes. *Annu. Rev. Neurosci.* 8:369–406.

Ram, J. L., and D. Dagan. 1987. Inactivating and non-inactivating outward current channels in cell-attached patches of *Helix* neurons. *Brain Res.* 405:16–25.

Sakmann, B., and E. Neher, editor. 1983. *Single Channel Recording.* Plenum Press, New York. 503 pp.

Serrano, E. E. 1982. Variability in molluscan neuron soma currents. Ph.D. dissertation, Stanford University.

Siegelbaum, S. A., J. S. Camardo, and E. R. Kandel. 1982. Serotonin and cyclic AMP close single K^+ channels in *Aplysia* sensory neurons. *Nature (Lond.).* 299: 413–417.

Sigurdson, W. J., C. E. Morris, B. L. Brezden, and D. R. Gardner. 1987. Stretch activation of a K^+ channel in molluscan heart cells. *J. Exp. Biol.* 127:191–209.

Snedecor, G. W. 1956. Statistical Methods. Iowa State University Press, Ames, IA. 534 pp.

Solc, C. K., W. N. Zagotta, and R. W. Aldrich. 1987. Single channel and genetic analyses reveal two distinct A-type potassium channels in *Drosophila. Science (Wash. DC).* 236:1094–1098.

Standen, N.B. 1975. Calcium and sodium ions as charge carriers in the action potential of an identified snail neurone. *J. Physiol. (Lond.).* 249:241–252.

Stewart, W. W. 1978. Functional connections between cells as revealed by dye-coupling with a highly fluorescent naphthalimide tracer. *Cell.* 14:741–759.

Strickholm, A. 1961. Impedance of a small electrically isolated area of the muscle cell surface. *J. Gen. Physiol.* 44:1073–1088.

Strong, J. A., and L. K. Kaczmarek. 1986. Multiple components of delayed potassium current in peptidergic neurons of *Aplysia:* modulation by an activator of adenylate cyclase. *J. Neurosci.* 6:814–822.

Stuhmer, W., W. Roberts, and W. Almers. 1983. The loose patch clamp. *In* Single-Channel Recording. B. Sakmann, and E. Neher, editors. Plenum Press, New York. 123–132.

Tauc, L. 1962a. Site of origin and propagation of spike in the giant neuron of *Aplysia. J. Gen. Physiol.* 45:1077–1097.

Tauc, L. 1962b. Identification of active membrane areas in the giant neuron of *Aplysia. J. Gen. Physiol.* 45:1099–1115.

Taylor, P. S. 1987. Selectivity and patch measurements of A-current channels in *Helis Aspersa* neurones. *J. Physiol. (Lond.).* 388:437–447.

Thompson, S. H. 1977. Three pharmacologically distinct potassium channels in molluscan neurons. *J. Physiol. (Lond.).* 265:465–488.

Thompson, S., and J. Coombs. 1988. Spatial distribution of Ca currents in molluscan neuron cell bodies and regional differences in the strength of inactivation. *J. Neurosci.* 8:1929–1939.

Thompson, S., S. J. Smith, and J. W. Johnson. 1986. Slow outward tail currents in molluscan bursting pacemaker neurons: two components differing in temperature sensitivity. *J. Neurosci.* 6:3169–3176,

Westerfield, M., and H. D. Lux. 1982. Calcium-activated potassium conductance noise in small neurons. *J. Neurobiol.* 12:507–517.